3132 *Macromolecules* **2010**, *43*, 3132–3135
DOI: 10.1021/ma100066e

Macromolecules
COMMUNICATION TO THE EDITOR

Alignment of Self-Assembled Structures in Block Copolymer Films by Solvent Vapor Permeation

Chinedum O. Osuji*

Department of Chemical Engineering, Yale University, New Haven Connecticut

Received January 11, 2010
Revised Manuscript Received February 21, 2010

Chemical dissimilarity between or among contiguous monomer sequences of a block copolymer (BCP) chain drives demixing with the length scale of the resulting structure determined by a minimization of interfacial energy concurrent with a maximization of chain entropy described by end-to-end distance statistics. This simple yet elegant display of mesoscale self-assembly has motivated an intense interest in practically all aspects of BCP behavior. There is no shortage of compelling applications envisaged, but utilization of BCPs in areas of promise remains largely underdeveloped by comparison to our understanding of their physics and control of their chemistry.[1,2] The critical limitation in this context is the inability to control their self-assembly over large length scales, using facile methods that are well suited to the intended applications. Whether for use as photonic band gap materials,[3−5] templates for advanced lithography,[6−10] or membranes in energy applications,[11,12] a crucial and still unfulfilled requirement is for the production of single-crystal or near-single crystal quality materials using methods compatible with the desired end use, that is, the production of materials with long-range order and precisely controlled orientation of their nanoscale structure. Significant efforts have focused on developing methods to accomplish this goal. To date, directed self-assembly of BCPs has been advanced using shear flow, electric fields, magnetic fields, thermal gradients, and surface forces in thin films, as recently comprehensively reviewed.[13] Significant attention has been given to developing routes to achieve vertical alignment of self-assembled lamellar and cylindrical microdomains in BCP films. Such assemblies have long recognized potential in a broad range of applications in addition to those discussed formerly. In particular, they are highly sought for use as nanoporous membranes for chemoselective transport and size-selective separations.[14] Microdomains are known to assemble spontaneously in this vertical arrangement because of the influence of surface forces but only in films that are typically on the order of 1 μm or less in thickness.[15] Nonetheless, the potential for these ordered arrays of self-assembled structures is outstanding.

Here we present a novel method, solvent vapor permeation (SVP), for facile alignment of self-assembled structures in BCP films well in excess of the above-mentioned thickness limit. The technique is based on pressure-driven transport of a solvent in the vapor phase through a polymer film, resulting in long-range order and alignment of the BCP interfaces parallel to the vapor flux. Alignment can be achieved over large (millimeter scale) areas on relatively short time scales of 1 h. The approach is suitable for the processing of relatively thick films with thicknesses on the order of 1 mm. Here we demonstrate the formation of vertically aligned hexagonally packed cylinders on vapor permeation from an initially isotropic sample. This approach should be of broad utility and enables the realization of such vertically aligned cylinders or "standing cylinders" in mechanically robust BCP films.

The process is quite straightforward and is illustrated schematically in Figure 1. A BCP film of 0.5 to 0.7 mm thickness is mounted on the inner surface of a solvent impermeable vial cap. A drop of solvent such as tetrahydrofuran (THF) or toluene is used to fix the film to the cap, which has a circular opening of about 4−6 mm in diameter that is completely covered by the film. The vial is loaded with 4 mL of toluene, and the cap is tightly affixed. The sample is then placed in a temperature-controlled chamber, and the solvent is allowed to evaporate. The escape of the solvent occurs via permeation of its vapor through the polymer film, which is maintained at the same temperature as the vapor itself.

The polymer used for this study is a triblock copolymer containing a rubbery midblock composed of a random copolymer of ethylene and butylene and two glassy poly(styrene) end blocks, poly(styrene-*b*-ethylene/butylene-*b*-styrene) or SEBS. These materials are thermoplastic elastomers known by the trade name Kraton. The molecular weight was 118 kg/mol, and the styrene weight fraction was 0.29. The SEBS and all solvents were obtained from Aldrich Chemical and were used as received. The polymer film was initially prepared by slow solvent casting of a 10 wt % toluene solution at room temperature in a large flat dish. Toluene is a fairly good solvent for both the rubbery and glassy components with a solubility parameter of $\delta = 8.9\ (\mathrm{cal \cdot cm^{-3}})^{1/2}$ compared with 8.7 for PS and ~8.0 for ethylene/butylene.[16] Morphology was studied using small-angle X-ray scattering (SAXS) using Cu Kα radiation at a wavelength of $\lambda = 1.5405$ Å. The scattering vector q is defined as $q = (4\pi/\lambda)\sin(\theta)$, where the scattering angle is 2θ. The d spacing is given by $2\pi/q$. The resulting films displayed the expected morphology for this composition, hexagonally packed cylinders, as deduced from the as-cast SAXS data of Figure 2. The peaks in the scattering occur at scattering vector ratios of $1:3^{1/2}$ that are characteristic of the hexagonally packed cylinder structure. The primary reflection is at $q = 0.206\ \mathrm{nm^{-1}}$ corresponding to a d spacing of 30.5 nm. For hexagonally packed cylinders, the d spacing is related to the intercylinder distance, d_0, as $d_0 = (4/3)^{1/2}d$, and the volume fraction $\phi = (2\pi/\sqrt{3})(r/d_0)_2$. Using bulk densities of 1.05 and 0.92 g/cm^3 for poly(styrene) and poly(ethylene/butylene), respectively, $\varphi_{PS} = 0.26$, from which we deduce that the spacing between the cylinders is 35.2 nm and the cylinder radius is 9.4 nm.

Samples were subject to toluene vapor permeation at two temperatures, 65 and 140 °C. In the first case, solvent evaporation was concluded over ~8 h, whereas it was complete within 1 h at 140 °C. Additionally, a third film was subjected to vapor permeation at 140 °C as well as to a reduction in the atmospheric pressure on the exterior of the system of 250 mmHg or ~33 kPa using a vacuum pump. Figure 2 shows the integrated scattering intensity with the X-rays incident along the direction of the prior vapor permeation for these two samples. The data show that the as-cast morphology of hexagonally packed cylinders was maintained. For the 65 °C sample, there was no significant change in the scattering, with the primary reflection maintained at $q_0 = 0.206\ \mathrm{nm^{-1}}$. There is a slight increase in the scattered intensity at higher scattering vectors, suggesting some small improvements to the order in the system. By contrast, the sample subjected to vapor permeation at 140 °C shows significantly improved ordering after just 1 h. This is marked by the emergence of several

*Corresponding author. E-mail: chinedum.osuji@yale.edu.

 Published on Web 03/05/2010

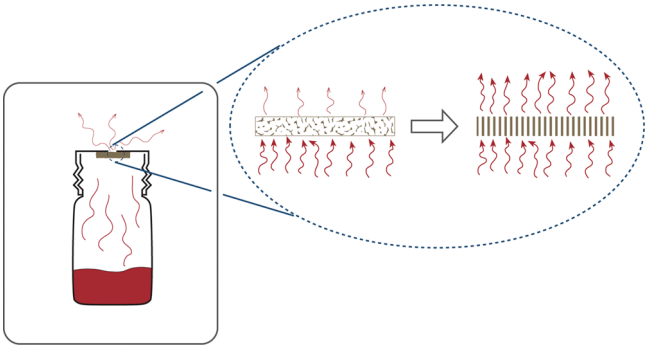

Figure 1. Schematic illustration of the experimental setup and of alignment of BCP domains via solvent permeation though the polymer film.

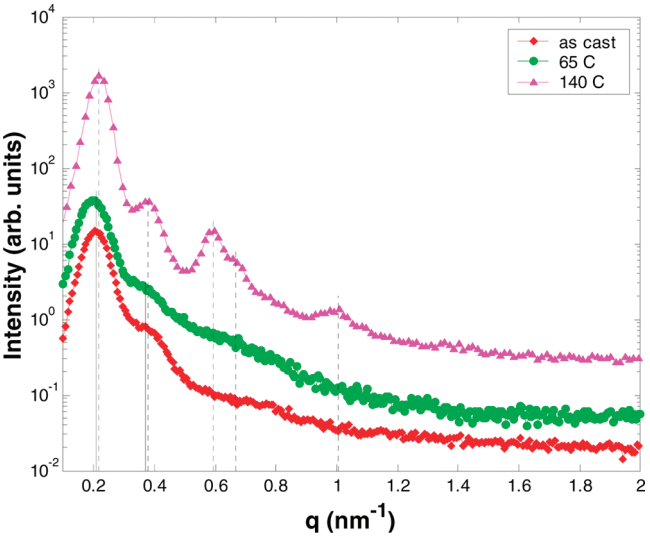

Figure 2. Integrated SAXS intensity for as-cast SEBS film and films subject to toluene vapor permeation at 65 and 140 °C. Peak locations are shown by the solid lines for as-cast and 65 °C samples and by dotted lines for the 140 °C sample. Data are shifted vertically for clarity.

clearly visible higher order peaks. They occur at q-squared ratios $(q/q_0)^2$ = 1:3:7:9:21 that are again characteristic of hexagonally packed cylinders. The primary reflection occurs at q_0 = 0.2171 nm^{-1} corresponding to a d spacing of 28.9 nm. This slight reduction in the d spacing is consistent with observations of sheared BCP solutions where decreases in the lamellar period are attributed to suppression of lamellar fluctuations at high shear rates.[17] The scattering intensity is sharply suppressed in the vicinity of q = 0.502 nm^{-1} and later at 0.905 nm^{-1}. These locations correspond to form factor minima for the cylindrical poly(styrene) microdomains, and the first is responsible for the typical loss of the $(q/q_0)^2$ = 2 or "root four" peak in hexagonally packed cylinders. The structure factor for semi-infinite rigid rods scales as $J_1(qR)/qR$, where J_1 is the Bessel function of the first kind.[18] Minima in this structure factor give rise to the minima in the cylinder form factor in the scattering from assemblies of cylinders. The first three solutions occur for (qR) = 3.8317, 7.01559, and 10.1735. On the basis of this, we calculate radii of 7.63 and 7.75 nm for the cylinders. It is unclear why these calculated radii are disproportionately smaller than the reduced d spacing when compared with the as-cast films. The scattering data are unambiguous, however in the indication of significantly improved long-range order in the system.

In Figure 3, 2-D SAXS data are shown for all three samples for X-rays incident parallel and perpendicular to the direction of the vapor flux, as shown in the schematic. The X-rays sample a circular area of roughly 0.5 mm diameter. In the parallel geometry, the entire film thickness is sampled. In the orthogonal geometry, the films were cut such that a thickness of roughly 1.5 mm is sampled. The data are thus statistically relevant because they represent the sampling of the BCP structure over quite large length scales relative to the d spacing of the system. For the sample prepared at 65 °C, no difference is observed between the two scattering patterns. By contrast, for both samples prepared at 140 °C, the orthogonal view shows the scattered intensity heavily concentrated along the equatorial direction, indicative of a well aligned morphology in which the long axes of the cylindrical microdomains are parallel to the prior vapor flux. In the parallel view, the scattering is isotropic because the uniaxial flow field of the solvent vapor, as expected, does not influence the in-plane order of the hexagonal packing. Figure 4 shows the integrated SAXS intensity from the perpendicular views of the atmospheric pressure versus vacuum assisted preparations at 140 °C. No significant difference is observed, and both samples display the same long-range order and deep form factor minima observed in the parallel direction.

From the azimuthal angular dependences of the scattered intensities of the primary reflections, we can quantify the degree of alignment using an orientation order parameter, $< P_2 >$, the coefficient of the second term of the orientation distribution function, as shown in eq 1, where φ is the azimuthal angle.

$$P_2 = \frac{\int_0^{\pi/2} I(q,\varphi)(3\cos^2\varphi - 1)\sin\varphi \, d\varphi}{\int_0^{\pi/2} I(q,\varphi)\sin\varphi \, d\varphi} \quad (1)$$

For perfectly aligned structures, the order parameter is equal to 1, whereas isotropically distributed orientations yield an order parameter of 0. The order parameters for the aligned SEBS samples calculated in this way are 0.41 and 0.26 for the sample under atmospheric pressure and 250 mmHg reduced atmospheric pressure, respectively, with full widths at half-maximum of 18 and 35°. The order parameters in both cases indicate that the system is indeed aligned. It must be noted, however, that order parameter determination in this fashion is quite sensitive to artifacts that may be introduced by background subtraction.[19] The aligned cylinders are likely in coexistence with some fraction of unaligned material that contributes to an isotropic background at the scattering peak location, in addition to contributions from the experimental setup itself. To avoid ambiguity and to provide a baseline estimate, we calculate the order parameter without any background subtraction, although this results in an underestimation of the actual degree of alignment. A less susceptible measure is given simply by the full width at half-maximum of the azimuthal intensity. The origin of the difference in the alignment between the ambient and vacuum-assisted processes is unknown at this point. It may simply be a coincidence. Further studies are required to shed light on this.

The alignment produced in the samples is due to the pressure driven flow of the solvent vapor through the polymer film. We can calculate the temperature dependent solvent vapor pressure for toluene using the Antoine equation, eq 2,

$$\log P = A - \frac{B}{T + C} \quad (2)$$

where A = 6.955, B = 1344.8, and C = 219.482 for toluene,[20] pressure is in mmHg, and temperature is in degrees Celsius. At 65 °C, P = 22.2 kPa, compared with 215.4 kPa at 140 °C. The mobility of the polymer is expected to be dramatically higher at 140 °C than at 65 °C. In the absence of the permeating solvent, the glass-transition temperature of poly(styrene) is ~105 °C, and that of the ethylene/butylene midblock is about −35 °C. The average flux of solvent through the film is 6×10^{-3} mL·cm^{-2}·s^{-1} at

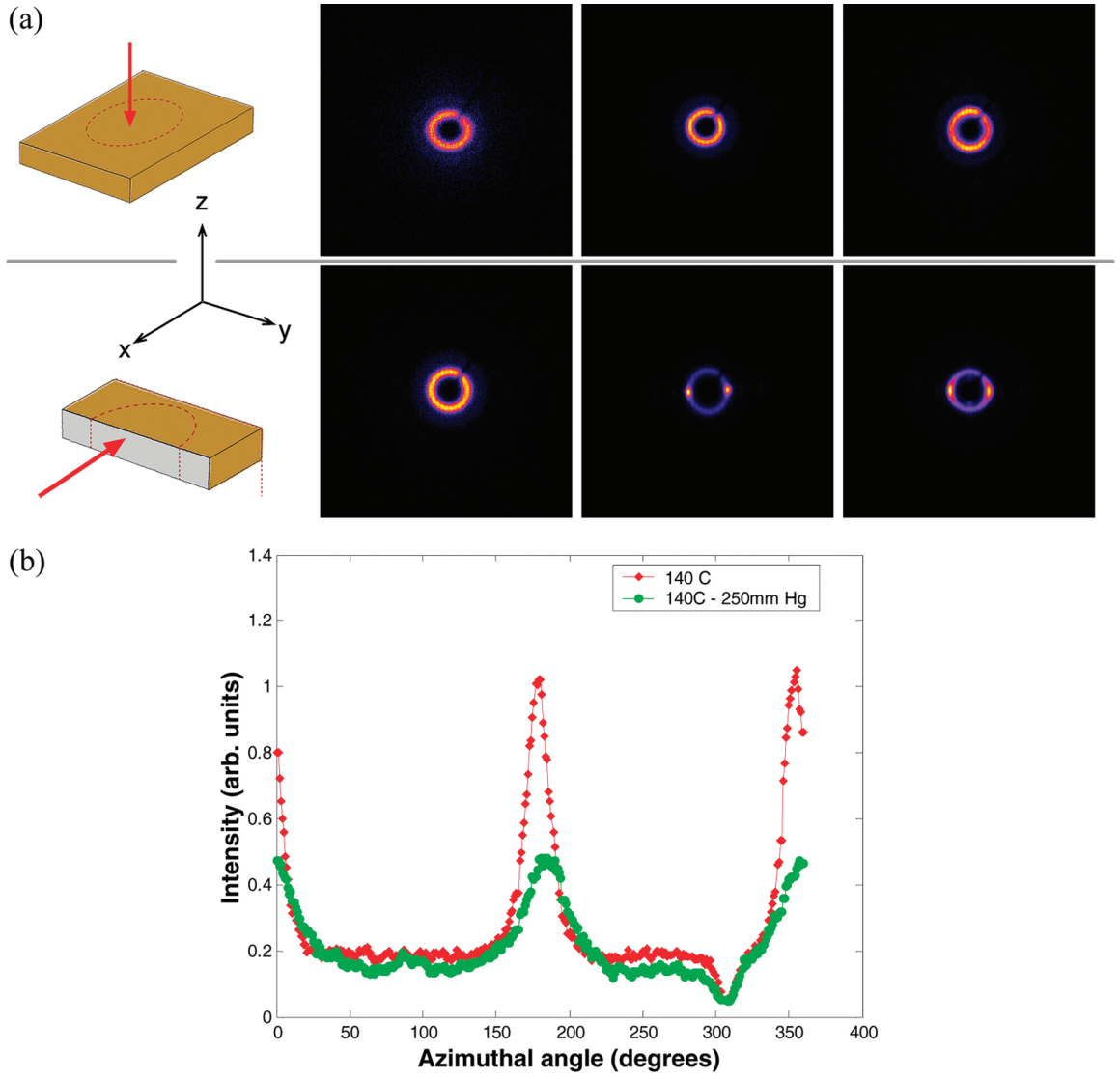

Figure 3. (a) Two-dimensional SAXS data for SEBS films subjected to vapor flux at 65 and 140 °C. The schematic shows the geometry of the scattering experiment with the red arrows denoting the incidence of X-rays. The dotted lines demark the area of the film exposed to permeation. Vapor flux is along the *z* axis. Top row: parallel geometry. Bottom row: perpendicular. Left to right: 65, 140, and 140 °C − 250 mmHg. Intensities are shown on logarithmic scale using a software derived color-mapping. (b) Azimuthal scattering intensity for 140 and 140 °C − 250 mmHg samples. The feature at 310° is due to the beam stop support of the instrument.

140 °C but only 7.5×10^{-4} at 65 °C. All of these variables certainly contribute to the difference in the morphologies produced at the two temperatures. The factor of 8 increase in the permeation time at 65 °C versus 140 °C is roughly proportional to the factor of 10 difference in the calculated toluene vapor pressure. We presume that the loss of solvent takes place entirely by permeation through the polymer film, but we cannot completely rule out inadvertent escape due to any inadequate sealing of the vials.

The use of solvent vapor to improve ordering and for producing alignment in BCP films has been widely reported. Solvent vapor annealing utilizes a reservoir of solvent vapor, typically at atmospheric pressure, to provide moderate swelling of a polymer film by condensed solvent molecules over an extended period of time.[21,22] The increased mobility of the polymer in the swollen yet ordered state plays the same role as thermal annealing below the order−disorder transition but is less aggressive than high-temperature treatments. In situ experiments using GISAXS show that the process can be surprisingly fast and involves a rippling instability due to relaxation of coil conformations on solvent uptake.[23] Alignment of microstructure by solvent vapor relies on directional evaporation of the solvent from a swollen film and may simply represent the final part of a vapor annealing procedure.[24−28] In previous work, the rate of solvent evaporation has been identified as a critical factor in controlling the production of vertical versus in-plane structures in BCP thin films.[25] In that seminal work, solvent evaporation rates from about 1 to 200 nL/s were utilized, with fast evaporation (∼ 200 nL/s) leading to poorly ordered structures, intermediate rates (∼ 5 nL/s) producing vertically aligned cylinders, and the slowest rates (∼0.2 nL/s) resulting in an in-plane morphology. The flow rates estimated the rate of loss of solvent from the sample chamber overall during film casting, and do not necessarily represent the flow emanating from the polymer film itself. The flow rates in the current work are on the order of 1000 $nL \cdot cm^{-2} \cdot s^{-1}$ and provide an estimate of the average solvent flux directly through the film.

In both cases, vapor annealing as well as directional solvent evaporation, the resulting effects are limited to the near-surface region of the system and typically do not proceed beyond a depth of several hundred nanometers or 1 μm. Recent work has shown alignments produced in thick films of SEBS during the relaxation from a nonequilibrium spherical morphology to the equilibrium

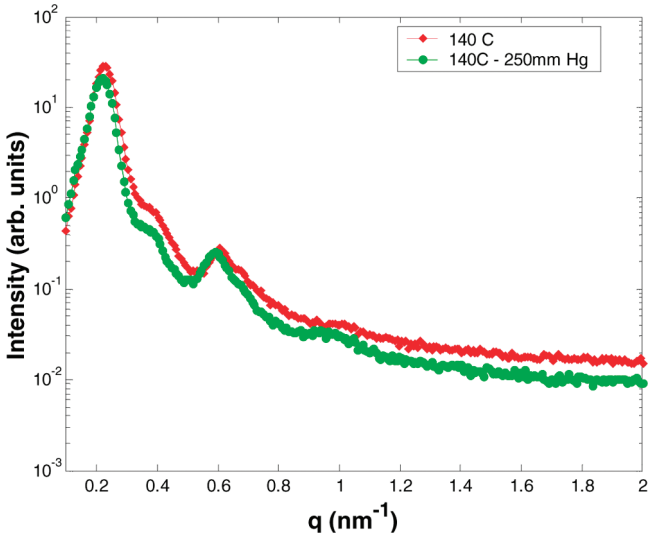

Figure 4. Integrated SAXS data along a direction perpendicular to the vapor flux for samples prepared at 140 °C.

cylinder structure.[28] The nonequilibrium morphology was induced by casting from a strongly selective heptane solution, prepared with the aid of dichloromethane. Coalescence of the spheres along a unique direction was reportedly due to memory of the chemical potential gradient induced by the original solvent evaporation. In the presently considered work, alignment is expressly due to the deliberate flux of solvent through the polymer film and does not involve a change of morphology or require a subsequent thermal anneal. It is a fast driven process, akin to the alignment induced by imposition of shear or extensional flows on swollen polymer melts. The polymer microstructure is aligned by the relative motion of solvent molecules past the polymer chains.

Whereas mechanical flow fields are highly effective at producing well-ordered and aligned BCP morphologies, their use for the alignment of films along the thickness direction is confounded by the inability to prescribe precisely shear or extensional forces in this geometry. The approach presented here effectively permits the application of a flow field in the thickness direction by imposing a flux of solvent vapor through the stationary film. It is important to decouple any possible effects due to bulk deformation of the system from those due to the solvent flux itself. In all cases considered here, the polymer film exhibited no discernible deformation (bending) due to the hydrostatic pressure imbalance imposed by the high solvent vapor pressure. Furthermore, by maintaining the entire sample under thermostatted conditions, as opposed to simply heating from the bottom, the vapor is not permitted to condense excessively into the polymer film and then vaporize at the exit surface. In previous experiments, such a setup produced unsatisfactory results because the films would often droop or even rupture as they lost mechanical integrity because of excessive swelling by condensed vapor. The imposition of a controlled temperature difference between the polymer film and the arriving vapor, however, may provide an additional means for controlling this process. In the current experiments, the pressure was defined simply by the liquid−vapor equilibrium of the solvent. Deliberate input of a pressurized externally provided vapor stream would represent an improvement to this. We note that attempts using hexane and methyl ethyl ketone, selective for the ethylene/butylene and styrene blocks, respectively, did not produce alignment at the temperatures used in this study. The nature of the solvent, along with the film thickness, solvent vapor pressure, and the temperatures of the vapor and film, represents a rich parameter space for further exploration.

In summary, we have demonstrated that a simple permeating flux of solvent vapor can be used to impart a well-defined orientation to microphase-separated BCP domains. Rapid, uniform alignment and long-range ordering of cylindrical microdomains was achieved in bulk films of 0.5 to 0.7 mm thickness on a time scale of just 1 h. This method appears to be well suited to the processing of BCP materials over relatively large areas. It facilitates the production of vertically aligned microdomains in mechanically robust films and thus may enable many promising and long-standing potential applications of BCP films with thicknesses beyond 1 μm. The influence of the controlling parameters remains to be explored in detail alongside the expected kinetic, morphological, and molecular weight effects. We expect that improvements in the alignments produced will result from such further studies.

Acknowledgment. The author thanks Pawel Majewksi and Manesh Gopinadhan for insightful discussions and help with setting up apparatus. This work was funded by the NSF under DMR-0847534.

References and Notes

(1) Hamley, I. W. *Angew. Chem., Int. Ed.* **2003**, *42*, 1692–1712.
(2) Park, C.; Yoon, J.; Thomas, E. L. *Polymer* **2003**, *44*, 6725–6760.
(3) Fink, Y.; Urbas, A. M.; Bawendi, M. G.; Joannopoulos, J. D.; Thomas, E. L. *J. Lightwave Technol.* **1999**, *17*, 1963–1969.
(4) Valkama, S.; Kosonen, H.; Ruokolainen, J.; Haatainen, T.; Torkkeli, M.; Serimaa, R.; Ten Brinke, G.; Ikkala, O. *Nat. Mater.* **2004**, *3*, 872–876.
(5) Osuji, C.; Chao, C. Y.; Bita, I.; Ober, C. K.; Thomas, E. L. *Adv. Funct. Mater.* **2002**, *12*, 753–758.
(6) Bang, J.; Kim, S. H.; Drockenmuller, E.; Misner, M. J.; Russell, T. P.; Hawker, C. J. *J. Am. Chem. Soc.* **2006**, *128*, 7622–7629.
(7) Cheng, J. Y.; Ross, C. A.; Thomas, E. L.; Smith, H. I.; Vancso, G. J. *Adv. Mater.* **2003**, *15*, 1599–1602.
(8) Segalman, R. A.; Yokoyama, H.; Kramer, E. J. *Adv. Mater.* **2001**, *13*, 1152–1155.
(9) Cheng, J. Y.; Ross, C. A.; Chan, V. Z. H.; Thomas, E. L.; Lammertink, R. G. H.; Vancso, G. J. *Adv. Mater.* **2001**, *13*, 1174–+.
(10) Bita, I.; Yang, J. K. W.; Jung, Y. S.; Ross, C. A.; Thomas, E. L.; Berggren, K. K. *Science* **2008**, *321*, 939–943.
(11) Shin, C. K.; Maier, G.; Andreaus, B.; Scherer, G. G. *J. Membr. Sci.* **2004**, *245*, 147–161.
(12) Soo, P. P.; Huang, B. Y.; Jang, Y. I.; Chiang, Y. M.; Sadoway, D. R.; Mayes, A. M. *J. Electrochem. Soc.* **1999**, *146*, 32–37.
(13) Darling, S. B. *Prog. Polym. Sci.* **2007**, *32*, 1152–1204.
(14) Olson, D. A.; Chen, L.; Hillmyer, M. A. *Chem. Mater.* **2008**, *20*, 869–890.
(15) Fasolka, M. J.; Mayes, A. M. *Annu. Rev. Mater. Res.* **2001**, *31*, 323–355.
(16) *Polymer Handbook*, 4th ed.; John Wiley & Sons: New York, 2003.
(17) Hamley, I. W. *Colloid Interface Sci.* **2000**, *5*, 342–350.
(18) Hamley, I. W.; Castelletto, V. *Prog. Polym. Sci.* **2004**, *29*, 909–948.
(19) Mitchell, G. R.; Windle, A. H. *Developments in Crystalline Polymers*; Elsevier Applied Science Publishers: London, 1988; Vol. *2*.
(20) Lange, N. A. *Lange's Handbook of Chemistry*; McGraw-Hill: New York, 1979.
(21) Jung, Y. S.; Ross, C. A. *Adv. Mater.* **2009**, *21*, 2540–2545.
(22) Fukunaga, K.; Hashimoto, T.; Elbs, H.; Krausch, G. *Macromolecules* **2002**, *35*, 4406–4413.
(23) Papadakis, C. M.; Di, Z.; Posselt, D.; Smilgies, D.-M. *Langmuir* **2008**, *24*, 13815–13818.
(24) Turturro, A.; Gattiglia, E.; Vacca, P.; Viola, G. T. *Polymer* **1995**, *36*, 3987–3996.
(25) Kim, G.; Libera, M. *Macromolecules* **1998**, *31*, 2569–2577.
(26) Fukunaga, K.; Elbs, H.; Magerle, R.; Krausch, G. *Macromolecules* **2000**, *33*, 947–953.
(27) Kim, S. H.; Misner, M. J.; Xu, T.; Kimura, M.; Russell, T. P. *Adv. Mater.* **2004**, *16*, 226–231.
(28) Sakurai, S.; Bando, H.; Yoshida, H.; Fukuoka, R.; Mouri, M.; Yamamoto, K.; Okamoto, S. *Macromolecules* **2009**, *42*, 2115–2121.